JOURNAL OF PROPULSION AND POWER
Vol. 26, No. 3, May–June 2010

Characterization of Fine Nickel-Coated Aluminum Powder as Potential Fuel Additive

Shashank L. Vummidi,* Yasmine Aly,* Mirko Schoenitz,† and Edward L. Dreizin‡
New Jersey Institute of Technology, Newark, New Jersey 07102

DOI: 10.2514/1.47092

Oxidation, ignition, and combustion processes are studied and compared for a fine nickel-coated aluminum powder and reference uncoated aluminum powder with a similar particle size distribution. Oxidation is studied by thermogravimetry in argon–oxygen mixtures. Ignition processes are studied for powders coated on an electrically heated metal filament. Combustion is characterized in constant volume explosion tests. Both ignition and combustion experiments were performed in air. Thermogravimetric measurements showed selective oxidation of Ni at low temperatures, at which the oxidation of Al remains undetected. At higher temperatures, oxidation for both the nickel-coated and uncoated powders occurs in a characteristic stepwise process with individual oxidation steps associated with polymorphic phase changes in the growing alumina layer and with the growth of individual alumina polymorphs. The activation energies for individual oxidation steps appear to be unaffected by the Ni coating; however the oxidation occurs somewhat faster for the coated powder, indicating an increase in the preexponential coefficients in Arrhenius formulations describing the respective oxidation processes. Ignition kinetics for both coated and uncoated powders are similar; however, ignition is more readily detected and appears to be more violent for the coated powders. Finally, powder combustion experiments showed substantially reduced ignition delays and somewhat increased overall burn rates for the coated powders.

Introduction

METAL fuel additives to propellants, explosives, and pyrotechnic compositions help increase the energy density of respective formulations [1–3]. Among various metal additives, aluminum is used most widely due to its high combustion enthalpy and low cost [1,4]. Aluminum particles are coated with a thin protective oxide layer, so that the heterogeneous oxidation reaction leading to aluminum ignition is rate controlled by a relatively slow diffusion of aluminum and oxygen ions through this layer [5–8]. Respectively, extended ignition delays often present a bottleneck for the overall combustion rate of aluminum powders. In addition, the agglomeration of aluminum particles before ignition, in particular occurring in solid propellant formulations, results in further ignition delays and the incomplete combustion of metal particles [9,10]. One approach proposed to reduce ignition delays and increase the burn rate of aluminum powders is based on using nickel surface coatings [11–21]. Such coatings are produced using one of several chemical methods, including an electroless nickel plate solution for treating aluminum powder [22], using aluminum to reduce metals from solutions of its salts [23], and using a modified polyol process [24]. Limited information is currently available about the ignition and combustion processes for such nickel-coated aluminum powders. For example, it was reported that nickel-coated aluminum powders could be ignited on the surface of an electrically heated nickel–chromium filament whereas similar powders without such coating did not ignite [21]. Coated powders also exhibited a reduced ignition temperature compared to uncoated aluminum [21]. Burn rates for individual particles were reported to be unaffected by the Ni coating [21]; however, the bulk burn rates of the coated powders were reported to be greater than that of uncoated aluminum [18]. It was reported that Al–Ni intermetallic reaction is capable of supporting a flame in a cloud of coated Al–Ni powders aerosolized in inert gas [13]. Experiments with Ni-coated particles with sizes ranging from 32 μm to 1 mm levitated in various oxidizing environments and ignited with a laser beam were reported in [14–16]. Those experiments established that, for Ni-coated particles with thick coatings ($\sim$50 wt% of Ni), ignition is defined by reactions in the Ni–Al system and does not depend on the presence of an external oxidizer. A similar conclusion was made for large, 2.5 mm particles with Ni coatings comprising 29 and 58 wt% ignited under normal and microgravity conditions [19]. For finer particles and thinner coatings, the Ni–Al reaction was considered a critically important exothermic process assisting ignition; however, the role of selective oxidation of nickel or the effect of nickel on the oxidation of aluminum were not considered. Micron-sized particles with small bulk concentrations of Ni are expected to be used in practical energetic formulations, in which it is desirable to maximize the overall energy density of the fuel additives. Thus, heat release due to the intermetallic Al–Ni reaction may become comparable to or even smaller than the heat released due to the heterogeneous oxidation of aluminum. The rate of oxidation itself can be affected by the presence of the Ni coating instead of, or in addition to, the natural amorphous aluminum oxide coating present on surface of pure Al powders. The objective of the present study is to characterize heterogeneous reactions leading to ignition in fine Ni-coated aluminum powders. It is further desired to assess whether the presence of relatively small amounts of Ni affect ensuing particle combustion.

Materials

Nominally spherical aluminum powder coated with nickel manufactured by Technion—Israel Institute of Technology was used for this study. According to the manufacturer's specification, the material contained 5 wt% of nickel. The powder's nominal particle size was 9.5 μm. For comparison, experiments were also performed with nominally spherical aluminum powder supplied by Alfa Aesar. The particle size was specified to be in the range of 1–5 μm and the powder purity was 99.9%.

The particle shapes and coating morphology are illustrated in the scanning electron microscope (SEM) images shown in Figs. 1 and 2.

Received 8 September 2009; revision received 18 January 2010; accepted for publication 18 January 2010.

*Graduate Research Assistant, Department of Chemical, Biological and Pharmaceutical Engineering.

†Associate Research Professor, Department of Chemical Biological and Pharmaceutical Engineering. Member AIAA.

‡Professor, Department of Chemical Biological and Pharmaceutical Engineering. Associate Fellow AIAA.

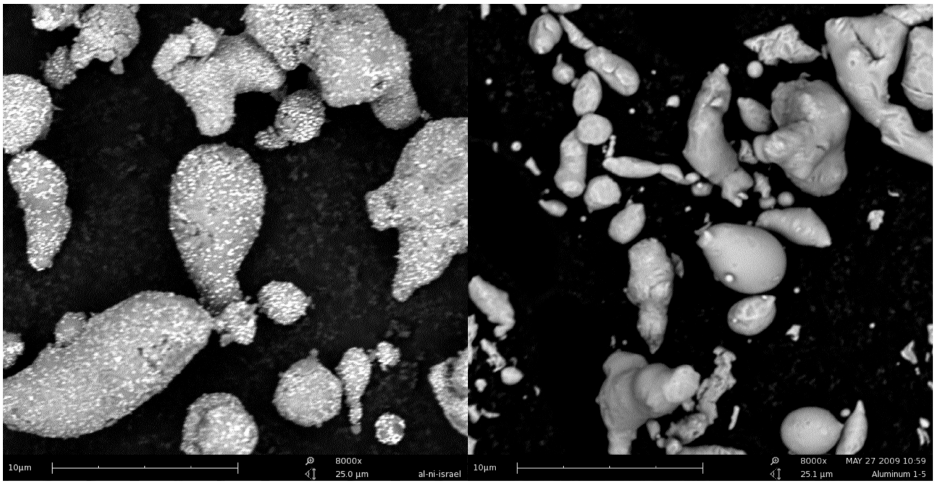

Fig. 1 SEM micrographs of powders of aluminum: a) coated with nickel, and b) uncoated.

An overview of the particle shapes is shown in Fig. 1 (using a Phenom Tabletop Microscope by FEI Technologies, Inc.). In both the nickel-coated and reference uncoated aluminum powders, multiple nonspherical particles are observed. Generally, the particle shapes and dimensions are similar between the two materials. Images obtained using backscattered electrons clearly show the nickel coating. The coating is not continuous; instead, it consists of multiple nickel particles adhering to the aluminum surface. Close-up, secondary electron images are shown in Fig. 2 (using a LEO 1530 Field Emission SEM), indicating that the nickel particles are nearly spherical, with sizes ranging approximately from 10 to 100 nm. The coating is not entirely uniform; some particles have surface spots without apparent coating. Note that a similar coating quality was reported in [21], in which powders prepared at Technion—Israel Institute of Technology were also used. In addition, a similar discontinuous coating was achieved in [24], in which a modified polyol process was used to prepare the powders. In most of the previous reports dealing with Ni-coated Al powders, the coating was reported to be continuous; however, the coating continuity was only directly confirmed for larger particles, for example, in [14,19]. Considering the morphology of the coating observed in this work as well as in [21,24], it is unclear whether a continuous Ni coating is achievable when fine Al particles are used and the mass percent of Ni is limited.

Particle size distributions were measured using a Beckman Coulter LS230 Enhanced Particle Analyzer and are presented in Fig. 3. The powders were suspended in deionized water. The laser scattering data was processed using a Mie scattering model with refractive indices taken from [25]. For both the nickel-coated and reference uncoated powders, the particle sizes are similar and the volume-based mean particle size in both cases is close to 9 μm. The similarities in particle size distributions and shapes justify the assumption that any differences in the oxidation, ignition, and combustion behaviors can be attributed to the role of the nickel coating.

X-ray diffraction (XRD) patterns for the nickel-coated powder were collected using a Philips X'pert MRD powder diffractometer operated at 45 kV and 40 mA and using unfiltered Cu K_α radiation (1.5438 Å). A characteristic pattern is shown in Fig. 4. The XRD patterns were used to assess the consistency within the powder batch used for the experiments. As expected, peaks of Al and Ni are observed with no major impurities or Al–Ni alloys detected. XRD patterns were collected from different powder samples to verify the consistency of the nickel concentration throughout the batch of powder used for the oxidation and combustion studies. The ratio of the amplitude of the Ni(200) peak to the sum of the amplitudes of the Ni(200) + Al(111) peaks calculated for different collected XRD patterns was found repeatedly to be at 0.0335 ± 0.0021 (standard deviation). The results were reproducible, indicating that the overall nickel concentration remained constant.

Experimental Techniques

The oxidation behavior of powders was studied using thermogravimetry (TG). The measurements were performed using a Netzsch Simultaneous Thermal Analyzer STA409 PC in a mixed Ar/O_2 environment. Flow rates of oxygen (Matheson Tri-Gas, 99.98%) and argon (Matheson Tri-Gas, 99.999%) were maintained at 50 ml/ min each. [To minimize the effect of coalescence of the molten aluminum particles on the reactive surface of the sample, selected experiments were performed with metallic powders blended with alumina. The alumina used was by Intramat Advanced Materials (α Al_2O_3, crystal size ~40 nm, particle size ~150 nm). To prepare samples for the TG measurements, 25 wt% of metallic material was added to 75 wt% of alumina; the powders were mixed in hexane using an ultrasonic bath. Before the TG measurements, the blended sample was dried in a vacuum chamber.] The TG experiments were repeated with both the blended and pure samples

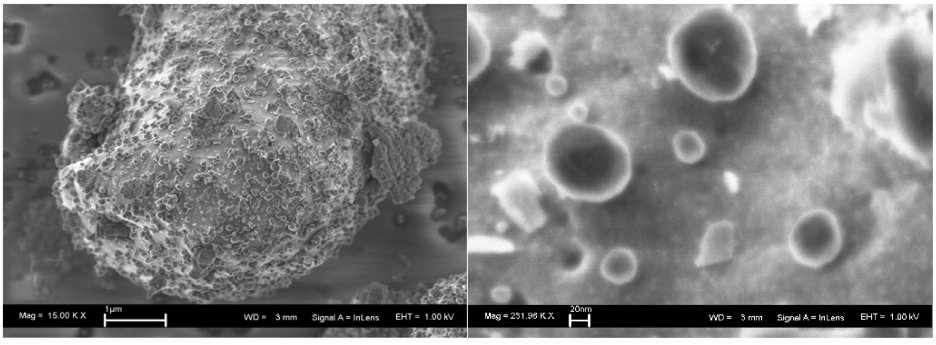

Fig. 2 Secondary electron SEM micrographs of a nickel-coated aluminum particle: a) overview, and b) close-up.

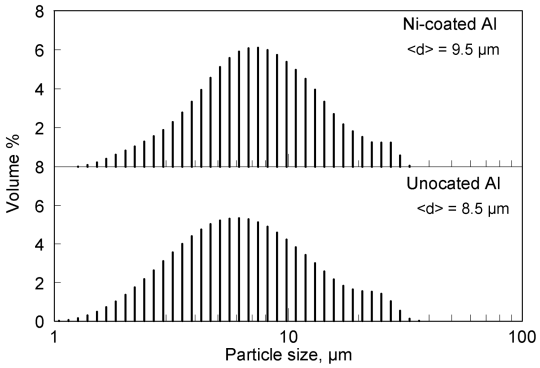

Fig. 3 Particle size distributions for the Ni-coated and uncoated aluminum powders.

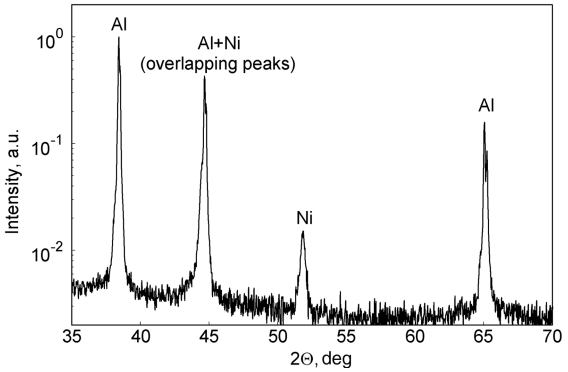

Fig. 4 X-ray diffraction pattern of the nickel-coated aluminum powder.

placed in the sample holder; the results were consistent between themselves indicating only a minor effect of the powder coalescence.

The ignition of materials was studied using a heated filament technique described in detail elsewhere [26–28]. A thin layer of powder was coated onto an electrically heated wire (alloy composition of 60% N, 16% Cr, and 24% Fe by Consolidated Electronic Wire and Cable; useful temperature range up to 1953 K or 1680°C). The wire temperature was monitored optically, while an additional photosensor recorded the emission from the powder coating. A spike or sudden increase in the powder emission intensity was interpreted as ignition, and the filament temperature at that instant was assumed to be the ignition temperature. Measurements performed at different filament heating rates enabled one to obtain information about the ignition kinetics. The filament ends are crimped into a spring-loaded holder, so that the filament remains straight despite its thermal expansion. However, when the temperature increases the filament becomes more and more ductile, and at some point it fails mechanically. In these experiments, it was noted that the heated filament failure often occurred at a temperature close to the ignition temperature of the powder coating. It was also noticed that, during the temperature ramp, some powder was falling off the filament, making detection of ignition of the remaining powder difficult. To remedy these issues, two heating wires were braided together and used as a heated filament. The braided wire was stronger than a single wire, so that its failure occurred at a higher temperature. Therefore, ignition was detected without interference with the signal produced by the failed filament. In addition, the powder coating adhered better to the braided wire surface.

Combustion of powders was characterized using a constant volume explosion (CVE) apparatus [29,30]. A cloud of powder was produced in a 9.2 l nearly spherical vessel; the cloud was ignited at its center by an electrically heated tungsten wire. A pressure transducer was used to record the pressure pulse produced by the propagating flame. The maximum pressure achieved in this CVE experiment is proportional to the total energy released in combustion, whereas the rate of pressure rise is indicative of the reaction rate. The CVE experiment is well suited for the comparison of combustion characteristics for different materials to each other, in this case comparing the combustion of coated and uncoated Al powders.

Results

Oxidation of Nickel-Coated Aluminum Powders

The weight increase during the oxidation of the Ni-coated aluminum powder and uncoated reference sample is shown in Fig. 5. Temperature derivatives of the recorded TG traces are also shown for both materials. The overall shapes of the TG traces are similar and exhibit a characteristic stepwise oxidation pattern as reported for aluminum earlier [5]. However, the first oxidation step for aluminum is preceded by a small weight increase occurring for the Ni-coated powder observed in the vicinity of 680 K. This weight increase is emphasized in the insets shown in Fig. 5 for both the TG traces and their derivatives. Following this small weight increase, the first oxidation step occurs identically for both the coated and uncoated powders. There are minor differences in the completeness of oxidation by the end of the second oxidation step, with the Ni-coated sample oxidizing slightly more than its uncoated counterpart. By the end of the third oxidation step, these differences diminish. There are also minor differences in the oxidation rates during the second and third oxidation steps, which are further explored in experiments with different heating rates.

The small weight increase at low temperatures was expected to be due to the selective oxidation of Ni. To validate this hypothesis, a sample of the Ni-coated powder was heated in the oxidizing environment in the TG analyzer to the temperature of 798 K (525°C), cooled off, and investigated by XRD. The obtained XRD pattern shown in Fig. 6 reveals the presence of nickel oxide (NiO) and the absence of metallic Ni, thus confirming that the initial, low-temperature weight increase was associated with the selective oxidation of Ni. Based on the Ni-peak-to-noise ratio in Fig. 4, and based on the noise measured in the XRD pattern shown in Fig. 6, it is concluded that less than 0.5% of Ni (less than one-tenth of the original nickel content) could remain undetected by the XRD measurement. The magnitude of the observed weight increase is also consistent with the hypothesis of the selective nickel oxidation. Oxidation of all the nickel present in the sample should result in about a 1.4% increase in the sample weight. The observed weight increase is about 2.4%, which indicates that the nickel is likely to be completely oxidized in addition to some additional low-temperature oxidation of the aluminum. No aluminum oxide phases are observed in the XRD patterns, however. This is not unusual for aluminum powder oxidation typically resulting in the formation of amorphous oxide.

TG experiments were performed at heating rates of 5, 20, and 40 K/ min to establish kinetics of each observed oxidation step. The derivatives of the recorded TG traces were obtained, and the peak positions were plotted in Arrhenius coordinates to recover respective apparent activation energies. It is of primary interest whether any of the oxidation steps observed at low heating rates in the TG

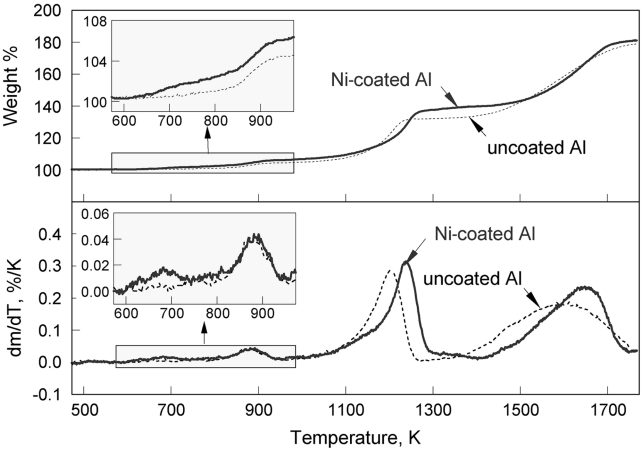

Fig. 5 TG traces and their derivatives for the oxidation of aluminum coated with nickel and uncoated aluminum powders.

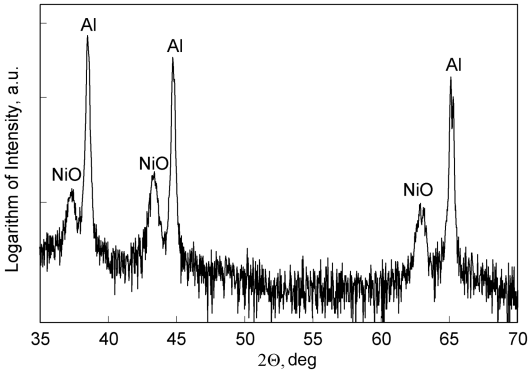

Fig. 6 XRD trace for the Ni-coated Al powder sample heated to 798 K (525°C) in an oxidizing environment at 5 K/min and cooled off.

experiments can be directly associated with the ignition of respective powders occurring at significantly greater heating rates. These results are presented in the next section, in comparison to the results of the heated filament ignition experiments.

The overall oxidation completeness was monitored for all TG experiments. The oxidation completeness for aluminum achieved for different heating rates can be compared between the two materials assuming that Ni is completely oxidized. With this assumption, supported by our observations presented earlier, for the Ni-coated material, the completeness of aluminum oxidation (a function Ψ, varied from 0 for unoxidized metal to 1 for the fully oxidized aluminum) can be evaluated based on the measured sample mass, m, and its initial mass, m_{initial}:

$$\Psi = \left(1 - \frac{m - m_{\text{initial}} \cdot \text{wt}\%_{\text{Ni}} \frac{\text{MW}_{\text{NiO}}}{\text{MW}_{\text{Ni}}}}{m_{\text{initial}} \cdot \text{wt}\%_{\text{Al}}}\right) \frac{1}{1 - \frac{\text{MW}_{\text{Al}_2\text{O}_3}}{2\text{MW}_{\text{Al}}}}$$

where wt% stand for weight percents and MW are the molecular weights with subscripts indicating individual species. The results comparing the oxidation completeness of Al for coated and uncoated powders for different heating rates are presented in Fig. 7.

Based on the total weight gain achieved, for all experimental heating rates the aluminum component in the Ni-coated samples was oxidized more completely than the uncoated aluminum.

Powder Ignition

Examples of characteristic sets of signals recorded in a filament ignition experiment are shown in Fig. 8. The temperature trace shown for each case is labeled as "extrapolated temperature" and is a temperature vs time dependency obtained by a linear extrapolation of the temperature ramp measured by the infrared pyrometer within its range of calibration, that is, 873–1203 K (600–930°C). The linear extrapolation is supported by calculations of the filament temperature based on the applied voltage, the impedance of the

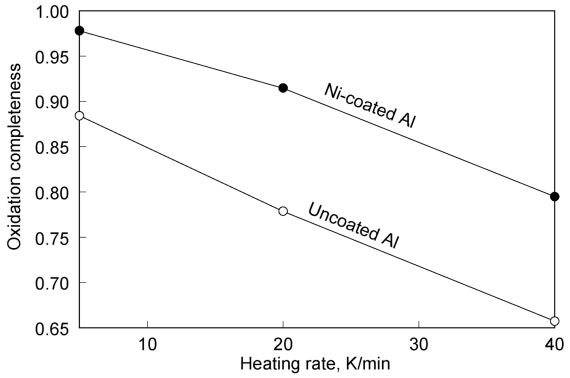

Fig. 7 Relative oxidation completeness for aluminum based on the final weight gain for the Ni-coated and uncoated Al samples heated to 1768 K (1495°C) in an oxidizing environment at different heating rates.

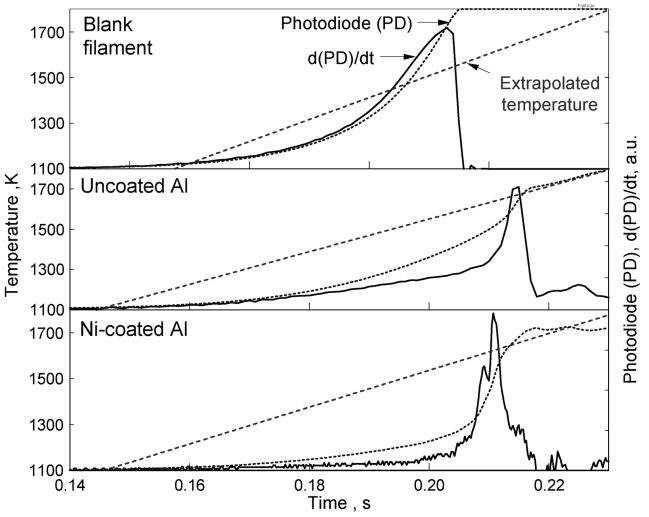

Fig. 8 Photodiode traces and their time derivatives used to identify ignition instant for the powders coated onto an electrically heated filament. For reference, similar traces recorded for a blank (uncoated) filament are also shown. In addition, temperature as a function of time is shown for each experiment. The temperature traces are obtained by extrapolation of the filament temperature as a function of time measured optically in the range of 600–930°C.

filament-containing circuit, and the heat transfer between the filament and surrounding air [26], and it remains valid while the radiation heat losses from the heated filament are small compared to convection. In a previous work [27], the linear extrapolation of the temperature ramp was also supported by additional temperature measurements using a three-color pyrometer. Despite nominally identical initial settings, the temperature ramps are not exactly the same for different repeated experiments; the differences between the temperature ramps shown in the three plots presented in Fig. 8 illustrate this. Primarily, the differences are due to the minor changes in the filament resistance and somewhat varied battery capacity (as it discharges in the course of experimentation).

The recorded photodiode traces initially exhibit an increase in the amplitude as expected for radiation of a gray body with a linearly increasing temperature. The ignition instant is determined from the recorded photodiode trace, which indicates a rapid increase in the emission intensity. To identify such an instant more reliably, a time derivative of the recorded photodiode signal is obtained, as shown in Fig. 8. For the blank filament, the increase in the photodiode signal is continuous, until the signal saturates (as in the example shown in Fig. 8) or until the filament breaks down, depending on the aperture restricting the light reaching the photodiode. Typically, the aperture is chosen to better resolve the photodiode signal in the vicinity of the ignition event. In the example shown in Fig. 8, the filament breaks down at a much higher temperature than ignition is observed, so that the photodiode signal recorded for the uncoated filament saturates. Respectively, the peak observed for the derivative of the photodiode signal for the uncoated filament is superficial and is associated with the saturation of the photodiode output. The initial increase in the photodiode signal for the powder-coated filaments (for both the pure and Ni-coated Al powders) is slower than that for the uncoated filament. This is chiefly due to a lower emissivity of the powder coating as compared to the uncoated filament surface. A rapid increase in the photodiode voltage is observed for both experiments with the powder-coated filaments; this increase occurs well before the photodiode voltage saturates or before the filament breaks down and is also clearly registered as a peak in the photodiode derivative trace. Note also that the increase is more pronounced and the respective photodiode derivative peak is sharper for the Ni-coated Al powder as compared to the peak produced by igniting uncoated Al. After the powder ignition, the photodiode signal is strongly affected by combustion, so that the ignition instant and corresponding ignition temperatures are the only two parameters usefully recovered from such experiments.

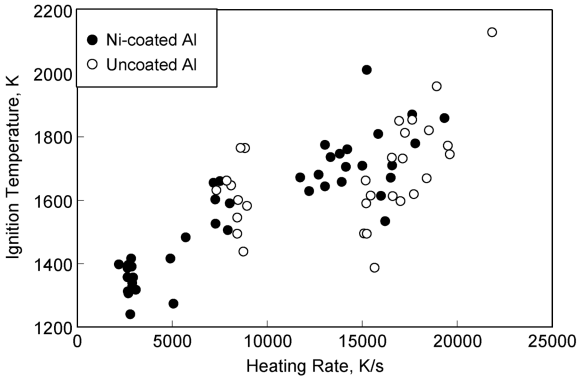

Fig. 9 Ignition temperature as a function of the heating rate for the Ni-coated and uncoated aluminum powders.

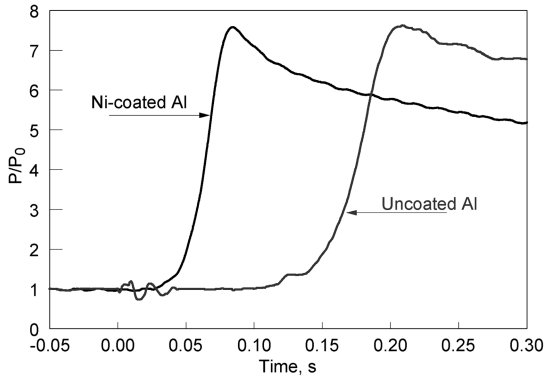

Fig. 10 Pressure traces (presented as ratio of the measured pressure over the initial pressure in the combustion vessel) obtained from the constant volume explosion experiments for the Ni-coated and uncoated aluminum powders.

The ignition temperatures measured for different heating rates for the nickel-coated Al powder are shown in Fig. 9. For reference, the ignition temperatures for uncoated Al are also shown. Note that, at heating rates below 8000 K/s, the ignition of uncoated Al could not be detected. At higher heating rates, the ignition temperatures practically coincide for both powders. A measurable increase in the ignition temperature as a function of the heating rate is detected despite a fairly significant spread of the experimental points. This trend, characteristic of a thermally activated process driving ignition, will be further discussed in comparison with the results of the TG experiments performed at varied heating rates.

Powder Combustion

Characteristic pressure traces recorded for the combustion of nickel-coated aluminum and pure aluminum powders in a constant volume vessel are shown in Fig. 10. Both powders ignite and burn producing similar maximum pressures and exhibiting generally similar rates of pressure rise. The main difference between the two materials appears to be in the induction period, which is the time after the igniter was initiated and until a substantial pressure increase was observed. This time can be interpreted as necessary to establish a self-propagating flame. To quantify the induction period, it was defined as the time between the ignition pulse and the instant when 10% of the maximum pressure is achieved. A summary of CVE results is shown in Fig. 11. Consistent with the observations made from Fig. 10, the values of achieved maximum pressure normalized by the initial pressure in the vessel, P_{max}/P_0, as well as the values of the maximum rates of pressure rise, dP/dt_{max}, are very similar for the coated and uncoated powders. A substantial difference is observed for the induction period, which is shorter for the Ni-coated material.

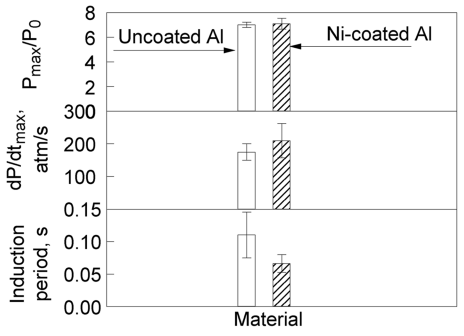

Fig. 11 Summary of the constant volume explosion experiment results for the Ni-coated and uncoated aluminum powders.

Discussion

A set of experiments presented in this paper compares side by side two aluminum powder samples, one of which is coated with a thin, discontinuous layer of Ni. The particle size distributions and particle shapes are generally similar for both powders, as illustrated in Figs. 1 and 2, so that the differences in the observed oxidation, ignition, and combustion behaviors can be unambiguously assigned to the effect of the Ni coating.

A characteristic stepwise aluminum oxidation process attributed earlier to polymorphic transitions in the protective Al_2O_3 layer [5] was observed to occur for both the Ni-coated and uncoated powders (cf. Figure 5). In the TG experiments with the Ni-coated powder, aluminum oxidation was preceded by selective oxidation of Ni. However, no effect of Ni coating or of the NiO produced later could be detected on the apparent activation energies assigned to the subsequent aluminum oxidation steps. A somewhat greater degree of oxidation detected for the Ni-coated sample (cf. Figure 7) heated to the same temperature as the uncoated materials at various heating rates suggests that the oxidation rate was indeed increased.

Ignition of the coated and uncoated samples on the heated filament also occurred in a qualitatively similar fashion. The most substantial difference between the samples was a more-pronounced radiation increase observed upon ignition of the Ni-coated samples (cf. Figure 8). This resulted in a more clearly identifiable ignition onset for all heating rates. The relatively mild increase in the photodiode signal upon ignition of the uncoated Al powder was undetectable for the lowest heating rate, whereas ignition of the Ni-coated samples could still be readily distinguished.

An increase in the heating rate resulted in an increase in the measured ignition temperature, as shown in Fig. 9, and no significant difference between the coated and uncoated powders was observed. The results of the TG experiments performed at different heating rates and processed using the Kissinger method [31] for each individual oxidation step are presented in Fig. 12, together with the filament ignition results processed in the same way. It is interesting that the group of experimental points obtained from the filament

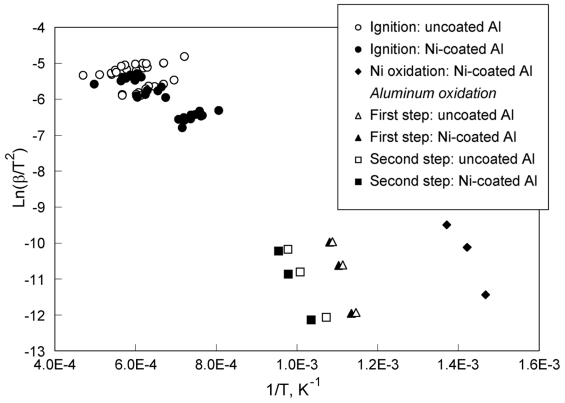

Fig. 12 Kissinger plot (logarithm of heating rate, β, corrected by the temperature square, $1/T^2$, vs the inverse temperature, $1/T$) comparing the results from the filament ignition and TG experiments for the Ni-coated and uncoated Al powders.

ignition measurements lines up best with the trend line formed by the points representing the second oxidation step of aluminum measured by the TG. This oxidation step is attributed to the growth of γ-Al_2O_3 that is rate limited by diffusion through the polycrystalline oxide film [5]. Oxidation processes occurring at lower temperatures, including the selective oxidation of Ni, the growth of amorphous aluminum oxide, and its transformation into γ-Al_2O_3, do not seem to be important for predicting the ignition temperatures of the aluminum powders studied. This observation suggesting the key role of kinetics of growth of γ-Al_2O_3 as controlling the particle ignition is equally relevant for both the Ni-coated and uncoated Al powders. Note that the latter conclusion may not remain valid if powders with very different particle sizes (e.g., nanopowders or very coarse particles) were used.

If the kinetics of growth of γ-Al_2O_3 (as well as the kinetics of ignition for aluminum powders) are described using conventional Arrhenius formalism, the results presented in Fig. 12 show that the apparent activation energies are effectively the same for the Ni-coated and uncoated powders. However, the preexponential factors do not have to be the same. In fact, minor differences observed in the completeness of oxidation for the two materials heated at the same rate to the same temperatures indicate a greater preexponent for the Ni-coated powder, which achieves greater oxidation completeness under the same heating conditions. The difference in the preexponent can be interpreted considering that the oxidative growth of γ-Al_2O_3 is controlled by the grain boundary diffusion, so that an increase in the preexponent can simply mean a reduction of the grain sizes and a corresponding increase in the number of grain boundaries. Additional grain boundaries can also be produced at the interfaces of Ni or NiO particles and Al or the Al_2O_3 surface.

An increase in the Arrhenius preexponent is also consistent with the observed, more-pronounced increase in the photodiode signal (and the respective peak in its derivative) accompanying ignition of the Ni-coated powders on the electrically heated filament (cf. Figure 8). Because ignition is observed at effectively the same temperatures for both the Ni-coated and uncoated powders, the difference in the preexponent must be relatively minor. Finally, a minor difference in the ignition preexponent and a somewhat more violent ignition can also explain the observed reduction in the induction time observed for the constant volume experiments with the Ni-coated powders (cf. Figure 11). Note that the heterogeneous oxidation processes driving ignition are replaced with a much more rapid, vapor-phase combustion when the particle temperature becomes sufficiently high. Therefore, the effect of the ignition kinetics on the overall burn rates is small.

In closing, it is interesting to briefly compare the present results with previous publications describing the ignition and combustion of Ni-coated aluminum particles. In most of the previous papers, large Al particles coated with continuous and rather thick layers of Ni were considered; see, for example, [13,14,19,20]. It was reported that for such samples, unlike for the powder used in this paper, the exothermic reaction resulting in the formation of a Ni–Al alloy was important in promoting ignition. Similar to this work, a discontinuous coating was detected for micron-sized particles with smaller Ni contents in [21]. The continuity of the Ni coating for smaller Ni concentrations was not directly confirmed for micron-sized particles in [15–18]; however, it was inferred that, similar to the coarser, Ni-clad particles, the Al–Ni intermetallic reaction plays a key role in triggering ignition of such materials. For the fine Al powders employed in this study, which were coated with a thin and discontinuous Ni layer, the intermetallic reaction was not detected. Instead, it was observed that Ni starts oxidizing at a lower temperature than Al and that, for both the Ni-coated and uncoated powders, oxidation is driven by processes with effectively the same activation energy, although with different preexponent factors. This consistent activation energy was attributed to the growth of the γ-Al_2O_3 polymorph, occurring for both the coated and uncoated Al powders, and was not associated with any reaction directly involving Ni or NiO. It is likely that the reaction mechanisms described in this study for fine, micron-sized powders coated with relatively small amounts of Ni are most relevant for the practical situations and systems in which such powders might be used.

Conclusions

The oxidation of fine aluminum powders coated by a discontinuous thin layer of nickel begins with the selective oxidation of nickel, which is followed by a characteristic sequence of growth and a polymorphic phase transformation in the aluminum oxide. For the micron-sized powders, the ignition is driven by growth of γ-Al_2O_3 for both the coated and uncoated materials. It appears that, despite the same activation energy for the ignition-driving oxidation process, the rate of oxidation is somewhat greater for the coated powders. The increased rate of heterogeneous oxidation reaction results in the greater degree of oxidation of Ni-coated powders under identical heating conditions, in shorter ignition delays, and in more-pronounced optical signatures produced by the igniting particles. The changes in the overall combustion energy released in constant volume explosion tests are negligible for the coated and uncoated powders.

The intermetallic Al–Ni reactions reported earlier that play a substantial role in improving ignition of Ni-clad Al particles of much greater dimensions and with greater Ni concentrations were not observed to occur for the micron-sized powders studied here.

Acknowledgments

This work was supported by Defense Threat Reduction Agency. The nominally spherical aluminum powder coated with nickel was provided for this study by V. Rozenband of Technion—Israel Institute of Technology.

References

[1] Price, E. W., and Sigman, R. K., *Combustion of Aluminized Solid Propellants*, Vol. 185, Progress in Astronautics and Aeronautics, AIAA, Reston, VA, 2000, p. 663.

[2] Grishkin, A. M., Dubnov, L. V., Davidov, V. Yu., Levshina, Yu. A., and Mikhailova, T. N., "Effect of Powdered Aluminum Additives on the Detonation Parameters of High Explosives," *Combustion, Explosion, and Shock Waves*, Vol. 29, No. 2, 1993, pp. 239–241. doi:10.1007/BF00755887

[3] Kubota, N., and Serizawa, C., "Combustion Process of Mg/TF Pyrotechnics," *Propellants, Explosives, Pyrotechnics*, Vol. 12, No. 5, 1987, pp. 145–148. doi:10.1002/prep.19870120502

[4] Beckstead, M. W., "Correlating Aluminum Burning Times," *Combustion, Explosion, and Shock Waves*, Vol. 41, No. 5, 2005, pp. 533–546. doi:10.1007/s10573-005-0067-2

[5] Trunov, M. A., Schoenitz, M., Zhu, X., and Dreizin, E. L., "Effect of Polymorphic Phase Transformation in Al_2O_3 Film on Oxidation Kinetics of Aluminum Powders," *Combustion and Flame*, Vol. 140, 2005, pp. 310–318. doi:10.1016/j.combustflame.2004.10.010

[6] Trunov, M. A., Schoenitz, M., and Dreizin, E. L., "Effect of Polymorphic Phase Transformation in Alumina Layer on Ignition of Aluminum Particles," *Combustion Theory and Modelling*, Vol. 10, No. 4, 2006, pp. 603–623. doi:10.1080/13647830600578506

[7] Eisenreich, N., Fietzek, H., Del Mar Juez-Lorenzo, M., Kolarik, V., Koleczko, A., and Weiser, V., "On the Mechanism of Low Temperature Oxidation for Aluminum Particles Down to the Nanoscale," *Propellants, Explosives, Pyrotechnics*, Vol. 29, No. 3, 2004, pp. 137–145. doi:10.1002/prep.200400045

[8] Park, K., Lee, D., Rai, A., Mukherjee, D., and Zachariah, M. R., "Size-Resolved Kinetic Measurements of Aluminum Nanoparticle Oxidation with Single Particle Mass Spectrometry," *The Journal of Physical Chemistry. B, Materials, Surfaces, Interfaces, & Biophysical*, Vol. 109, No. 15, 2005, pp. 7290–7299. doi:10.1021/jp048041v

[9] Sambamurthi, J. K., Price, E. W., and Sigman, R. K., "Aluminum Agglomeration in Solid-Propellant Combustion," *AIAA Journal*, Vol. 22, No. 8, 1984, pp. 1132–1138. doi:10.2514/3.48552

[10] Babuk, V. A., and Vasilyev, V. A., "Model of Aluminum Agglomerate Evolution in Combustion Products of Solid Rocket Propellant," *Journal of Propulsion and Power*, Vol. 18, No. 4, 2002, pp. 814–823. doi:10.2514/2.6005

[11] Breiter, A. L., Mal'tsev, V. M., and Popov, E. I., "Means of Modifying Metallic Fuel in Condensed Systems," *Combustion, Explosion, and Shock Waves*, Vol. 26, No. 1, 1990, pp. 86–92. doi:10.1007/BF00742280

[12] Yagodnikov, D. A., and Voronetskii, A. V., "Experimental and Theoretical Study of the Ignition and Combustion of an Aerosol of Encapsulated Aluminum Particles," *Combustion, Explosion and Shock Waves*, Vol. 33, No. 1, 1997, pp. 49–55. doi:10.1007/BF02671852

[13] Mukasyan, A. S., Lau, C., and Varma, A., "Gasless Combustion of Aluminum Particles Clad by Nickel," *Combustion Science and Technology*, Vol. 170, No. 1, 2001, pp. 67–85. doi:10.1080/00102200108907850

[14] Shafirovich, E., Mukasyan, A., Thiers, L., Varma, A., Legrand, B., Chauveau, C., and Gökalp, I., "Ignition and Combustion of Al Particles Clad by Ni," *Combustion Science and Technology*, Vol. 174, No. 3, 2002, pp. 125–140. doi:10.1080/713712997

[15] Escot Bocanegra, P., Chauveau, C., and Gökalp, I., "Experimental Studies on the Burning of Coated and Uncoated Micro and Nano-Sized Aluminium Particles," *Aerospace Science and Technology*, Vol. 11, No. 1, 2007, pp. 33–38. doi:10.1016/j.ast.2006.10.005

[16] Shafirovich, E., Escot Bocanegra, P., Chauveau, C., Gokalp, I., Goldshlegerb, U., Rosenband, V., and Gany, A., "Ignition of Single Nickel-Coated Aluminum Particles," *Proceedings of the Combustion Institute*, Vol. 30, 2005, pp. 2055–2062. doi:10.1016/j.proci.2004.08.107

[17] Rosenband, V., and Gany, A., "Activated Metal Powders as Potential Energetic Materials," *Advancements in Energetic Materials and Chemical Propulsion*, edited by K. K. Kuo, and K. Hori, Begell House, New York, 2008, pp. 838–854.

[18] Hahma, A., Gany, A., and Palovuori, K., "Combustion of Activated Aluminum," *Combustion and Flame*, Vol. 145, 2006, pp. 464–480. doi:10.1016/j.combustflame.2006.01.003

[19] Andrzejak, T. A., Shafirovich, E., and Varma, A., "Ignition of Iron-Coated and Nickel-Coated Aluminum Particles under Normal- and Reduced-Gravity Conditions," *Journal of Propulsion and Power*, Vol. 24, No. 4, 2008, pp. 805–813. doi:10.2514/1.34034

[20] Andrzejak, T. A., Shafirovich, E., and Varma, A., "Ignition Mechanism of Nickel-Coated Aluminum Particles," *Combustion and Flame*, Vol. 150, 2007, pp. 60–70. doi:10.1016/j.combustflame.2007.03.004

[21] Boyd, E., Houim, R., and Kuo, K. K., "Ignition and Combustion of Nickel Coated and Uncoated Aluminum Particles in Hot Post-Flame Environment," AIAA Paper 2009-5441, Aug. 2009.

[22] Ramaseshan, R., Seshadri, S. K., and Nair, N. G., "Electroless Nickel-Phosphorus Coating on Ti and Al Elemental Powders," *Scripta Materialia*, Vol. 45, No. 2, 2001, pp. 183–189. doi:10.1016/S1359-6462(01)01013-2

[23] Hahma A., "Modified Metal Powder and Method of Increasing the Bum Rate and Ignitability of a Metal Powder Fuel," European Patent Application, Publication SE527338 (C2) 2006.

[24] Cheng, J. L., Hng, H. H., Ng, H. Y., Soon, P. C., and Lee, Y. W., "Deposition of Nickel Nanoparticles onto Aluminum Powders Using a Modified Polyol Process," *Materials Research Bulletin*, Vol. 44, 2009, pp. 95–99. doi:10.1016/j.materresbull.2008.03.028

[25] Palik D. E., *Handbook of Optical Constants of Solids*, Academic Press, San Diego, CA, 1998.

[26] Ward, T. S., Trunov, M. A., Schoenitz, M., and Dreizin, E. L., "Experimental Methodology and Heat Transfer Model for Identification of Ignition Kinetics of Powdered Fuels," *International Journal of Heat and Mass Transfer*, Vol. 49, 2006, pp. 4943–4954. doi:10.1016/j.ijheatmasstransfer.2006.05.025

[27] Mohan, S., Trunov, M. A., and Dreizin, E. L., "Characterization of Aluminum Powder Ignition," *Chemical and Physical Processes in Combustion*, Combustion Inst., Pittsburgh, PA, 2003, pp. 329–332.

[28] Shoshin, Y. L., Trunov, M. A., Zhu, X., Schoenitz, M., and Dreizin, E. L., "Ignition of Aluminum-Rich Al–Ti Mechanical Alloys in Air," *Combustion and Flame*, Vol. 144, 2006, pp. 688–697. doi:10.1016/j.combustflame.2005.08.037

[29] Eapen, B. Z., Hoffman, V. K., Schoenitz, M., and Dreizin, E. L., "Combustion of Aerosolized Spherical Aluminum Powders and Flakes in Air," *Combustion Science and Technology*, Vol. 176, 2004, pp. 1055–1069. doi:10.1080/00102200490426433

[30] Trunov, M. A., Hoffmann, V. K., Schoenitz, M., and Dreizin, E. L. "Combustion of Boron–Titanium Nanocomposite Powders in Different Environments," *Journal of Propulsion and Power*, Vol. 24, No. 2, 2008, pp. 184–191. doi:10.2514/1.30483

[31] Kissinger, H. E., "Reaction Kinetics in Differential Thermal Analysis," *Analytical Chemistry*, Vol. 29, No. 11, 1957, pp. 1702–1706. doi:10.1021/ac60131a045

S. Son
Associate Editor